NASA Contractor Report 3154

Numerical Optimization Techniques for Bound Circulation Distribution for Minimum Induced Drag of Nonplanar Wings: Basic Formulations

John Kuhlman

GRANT NSG-1357
JUNE 1979

NASA

NASA Contractor Report 3154

Numerical Optimization Techniques for Bound Circulation Distribution for Minimum Induced Drag of Nonplanar Wings: Basic Formulations

John Kuhlman
Old Dominion University Research Foundation
Norfolk, Virginia

Prepared for
Langley Research Center
under Grant NSG-1357

NASA
National Aeronautics
and Space Administration

Scientific and Technical
Information Office

1979

SUMMARY

A theoretical method has been developed for determining the optimum span load distribution for minimum induced drag for subsonic nonplanar configurations. The undistorted wing wake is assumed to have piecewise linear variation of shed vortex sheet strength, resulting in a quadratic variation of bound circulation and span load. The optimum loading is obtained either through a direct technique, whereby derivatives of the drag expression are calculated analytically in terms of the unknown wake vortex sheet strengths, or through use of Munk's criterion. Both techniques agree well with each other and with available exact solutions for minimum induced drag.

INTRODUCTION

One way in which to improve aircraft performance at subsonic cruise is to utilize nonplanar lifting surfaces designed for minimum induced drag. At least two theoretical design methods have been developed for this purpose: one by Lamar (ref. 1) and another by Feifel (ref. 2). Ishimitsu (ref. 3) uses Feifel's technique for the design of winglets. Both of these theories use vortex lattice representations on the wing with trailing filaments extending streamwise into the wake. Feifel notes in reference 2 that the discretized vortex lattice technique can lead to appreciable errors in local velocity, and hence in the span load, for nonplanar configurations in the vicinity of an abrupt change in dihedral. Even though the effect on total coefficients is negligible, camber solutions in such regions can be in error. One way in which to minimize such problems is to assume a more complicated functional form of the bound circulation than piecewise constant. This avoids the isolated singularities of strength $(r)^{-1}$ which occur in vortex lattice representations, at the expense of more elaborate analysis. Three previously developed methods for improving the induced drag computation are those of Loth and Boyle (ref. 4), Goldhammer (ref. 5), and Clever (ref. 6).

Loth and Boyle developed a theoretical Trefftz plane analysis of the wake of a single planform where the wake vortex sheet strength was assumed piecewise linear and continuous. However, the numerical results from reference 4 are seriously in error due to errors in the implementation of this method. More recently Goldhammer and Clever have developed near-field analysis codes that assume piecewise linear variation of singularity strengths

in the chordwise direction. Reference 5 assumed a piecewise constant span load, leading to a discrete vortex representation of the wake, while reference 6 assumed a piecewise linear variation of span load, resulting in piecewise constant wake vortex sheet strengths. The current work utilizes the theoretical model developed by Loth and Boyle, where the shed sheet strength is assumed piecewise linear, leading to quadratic variations of bound circulation and span load.

A Trefftz plane analysis of a wing wake is performed using an assumed piecewise linear functional form of the wake strength, and solutions for the bound circulation for minimum induced drag are obtained using two optimization techniques. First, Munk's criterion (ref. 7), applied at each wake segment midpoint, is used, similar to the technique developed in reference 4, but with important analytic differences in the handling of singularities at the ends of adjacent wake segments and at the wing tips, as well as the inclusion of variable wake segment spacing. Second, a direct optimization technique as discussed in reference 1 is developed for the assumed wake model. Results for both techniques are then compared with available exact solutions from Mangler (ref. 8), Cone (ref. 9), Lundry (ref. 10), and Lundry and Lissaman (ref. 11).

SYMBOLS

$A_{p,k}$	matrix of coefficients in direct optimization technique
A,B,D,E,F,G,J,K,R,T,U,W A',D',F',G',J',K'	constants appearing in normal wash expression (eq. 4)
$A_{1_{ji}}$, $A_{2_{ij}}$, $A_{3_{ij}}$, $A_{4_{ij}}$	integrals appearing in normal wash expression (eq. 4)
b	wing span
C_L	lift coefficient
C_D	induced drag coefficient
d	vertical extent of circular arc
D_{ij}	induced drag on segment i due to induced velocity of segment j
$G_i, \bar{G}_i, \hat{G}_i$	variables containing unknown shed sheet strengths appearing in drag expression (eq. 7)

h_{ij}	distance between influenced point on segment i and influencing point on segment j
h'_{ij}	distance between influenced point on segment i and influencing point on image of segment j
$I1_{i,j}, I2_{i,j}, I3_{i,j}, I4_{i,j}, I5_{i,j}, I6_{i,j}$	integrals appearing in drag coefficient expression (eq. 7)
k	induced drag efficiency factor
K_1, K_2, K_3	constants appearing in integrals on p. 16 and p. 28
ℓ	vertical extent of endplate or fence
N_T	number of wake segments on one half of wing
P, Q	factors in normal induced velocity expressions
R_{ij}	projection of distance h_{ij} onto the plane of influenced segment i
R'_{ij}	projection of distance h'_{ij} onto the plane of influenced segment i
S_{ref}	reference wing area
δ	local wake segment coordinate
s	wake segment half width
U	free stream velocity
w	total induced velocity
w_n	normal wash velocity
$w^*_{n,j}$	normal wash velocity induced at point $\delta = \delta_i$ on segment i due to segment j
$w'_{n,j}$	normal wash velocity induced at point $\delta = \delta_i$ on segment i due to image of segment j
w_o	constant appearing in Munk's criterion normal wash velocity expression (eq. 8)
y	spanwise coordinate

z	vertical coordinate
$\beta = \frac{d}{b/2}$	parameter for circular arc spanwise camber
γ	trailing vortex sheet strength
Γ	bound circulation along the planform perimeter
$\bar{\Gamma}$	average bound circulation
η	nondimensional spanwise coordinate
λ	Lagrange multiplier
ρ	fluid density
σ_{ij}	angle between direction of h_{ij} and y-axis
ϕ	dihedral angle

Subscripts

i	influenced point
j	influencing point
n	normal component
p	dummy index
o	value at y = 0

Superscripts

'	image segment quantity
-	average quantity, or body axis coordinate

THEORETICAL DEVELOPMENT

To effect a solution for minimum induced drag using the assumed wake model, the standard expression for induced drag evaluated in the Trefftz plane, given by

$$C_D = \frac{1}{S_{ref}} \int_{-\frac{b}{2}}^{\frac{b}{2}} \frac{\Gamma}{U} \frac{w_n}{U} \frac{1}{\cos \phi} \, dy$$

can be used. To develop expressions for the individual quantities in the integrand, i.e. bound circulation and induced normal velocity in terms of the wake vortex sheet strength, consider a view from downstream of the undistorted wing wake as shown in figure 1. The wake is broken up into N_T linear segments which can be of varying size. Uniform and cosine segment spacing are investigated in the current study. From the law of Biot-Savart, the total induced velocity at a point on wake segment i, located a distance δ_i from the center of that segment, due to an increment of shed vorticity from segment j, located a distance δ_j from the center of that segment, is equal to

$$dw(\delta_i, \delta_j) = \frac{\gamma(\delta_j) d\delta_j}{2\pi h_{ij}}$$

where

$$h_{ij} = \left\{ (y_{ij} - \delta_j \cos \phi_j + \delta_i \cos \phi_i)^2 + (z_{ij} - \delta_j \sin \phi_j + \delta_i \sin \phi_i)^2 \right\}^{1/2}$$

and

$$y_{ij} = \bar{y}_i - \bar{y}_j; \qquad z_{ij} = \bar{z}_i - \bar{z}_j$$

Refer to figure 1 for details of geometry. The normal induced velocity is

$$dw_n^*(\delta_i,\delta_j) = dw(\delta_i,\delta_j) \quad \cos(\phi_i - \sigma_{ij})$$

$$= dw(\delta_i,\delta_j) \quad \frac{R_{ij}}{h_{ij}}$$

where σ_{ij} is the dihedral angle between points located distances δ_i and δ_j from the centers of segments i and j. R_{ij} is the projection of h_{ij} in the plane of segment i such that

$$R_{ij} = \sin\phi_i(z_{ij} - \delta_j \sin\phi_j + \delta_i \sin\phi_i)$$

$$+ \cos\phi_i(y_{ij} - \delta_j \cos\phi_j + \delta_i \cos\phi_i)$$

Thus, the normal wash at δ_i on segment i due to segment j is

$$w^*_{n,j}(\delta_i) = \frac{1}{2\pi}\int_{-s_j}^{+s_j} \frac{\gamma(\delta_j)\left\{\cos\phi_i(y_{ij} - \delta_j\cos\phi_j + \delta_i\cos\phi_i) + \sin\phi_i(z_{ij} - \delta_j\sin\phi_j + \delta_i\sin\phi_i)\right\}}{(y_{ij} - \delta_j\cos\phi_j + \delta_i\cos\phi_i)^2 + (z_{ij} - \delta_j\sin\phi_j + \delta_i\sin\phi_i)^2} d\delta_j \quad (1)$$

Next, consider the normal wash at a distance δ_i from the center of segment i due to the image of segment j, located on the right half of the wing. This normal wash, denoted by a prime, equals

$$dw'_n(\delta_i,\delta_j) = \frac{-\gamma(\delta'_j)d\delta'_j}{2\pi}\frac{\cos(\phi_i - \sigma'_{ij})}{h'_{ij}}$$

$$= \frac{-\gamma(\delta'_j)d\delta'_j}{2\pi}\frac{R'_{ij}}{[h'_{ij}]^2}$$

where

$$R'_{ij} = \sin\phi_i(z'_{ij} - \delta_j \sin\phi_j + \delta_i \sin\phi_i)$$

$$+ \cos\phi_i(y'_{ij} + \delta_j \cos\phi_j + \delta_i \cos\phi_i)$$

$$[h'_{ij}]^2 = (y'_{ij} + \delta_j \cos\phi_j + \delta_i \cos\phi_i)^2$$

$$+ (z'_{ij} - \delta_j \sin\phi_j + \delta_i \sin\phi_i)^2$$

The total induced normal wash at point i due to the image of segment j is then

$$w'_{n,j}(\delta_i) = \frac{-1}{2\pi} \int_{-s_j}^{+s_j} \frac{\gamma(\delta_j) \left\{ \cos\phi_i (y'_{ij} + \delta_j \cos\phi_j + \delta_i \cos\phi_i) + \sin\phi_i (z'_{ij} - \delta_j \sin\phi_j + \delta_i \sin\phi_i) \right\} d\delta_j}{(y'_{ij} + \delta_j \cos\phi_j + \delta_i \cos\phi_i)^2 + (z'_{ij} - \delta_j \sin\phi_j + \delta_i \sin\phi_i)^2} \quad (2)$$

where $y'_{ij} = \overline{y_i} + \overline{y_j}$ and $z'_{ij} = z_{ij}$. The normal wash at point i due to both segment j and its image, equal to $w^*_{n,j}(\delta_i) + w'_{n,j}(\delta_i)$, is then

$$w_{n,j}(\delta_i) = \frac{1}{2\pi} \int_{-s_j}^{+s_j} \gamma(\delta_j) \left(\frac{R_{ij}}{h_{ij}^2} - \frac{R'_{ij}}{(h'_{ij})^2} \right) ds_j .$$

The shed vorticity distribution, assumed piecewise linear as shown in sketch a, is defined for segment j as

$$\gamma(\delta_j) = \frac{\gamma_{j+1} + \gamma_j}{2} + \frac{\delta_j}{s_j} \cdot \frac{\gamma_{j+1} - \gamma_j}{2}$$

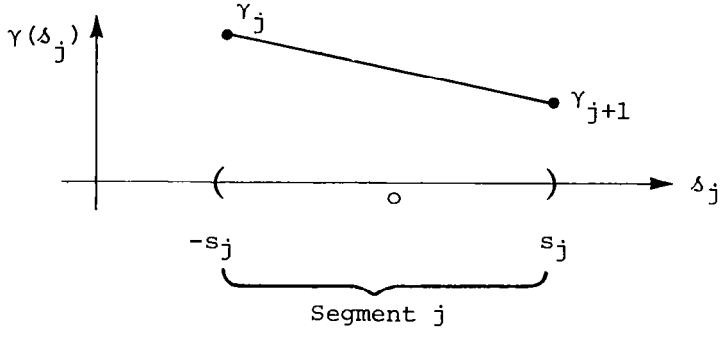

Sketch (a)

where γ_j is the value of the shed vorticity between segments j and $j-1$. The range of applicability of each equation for γ is $-s_j$ to s_j. Note that this assumption leads to piecewise quadratic distributions of bound circulation and span load.

Then the normal wash at δ_i due to segment j and its image is

$$w_{n,j}(\delta_i) = \frac{\gamma_{j+1} + \gamma_j}{2} \frac{1}{2\pi} \left\{ \int_{-s_j}^{+s_j} \frac{R_{ij} d\delta_j}{h_{ij}^2} - \int_{-s_j}^{+s_j} \frac{R'_{ij} d\delta_j}{[h'_{ij}]^2} \right\}$$

$$+ \frac{\gamma_{j+1} - \gamma_j}{2} \frac{1}{2\pi} \left\{ \int_{-s_j}^{+s_j} \frac{\delta_j R_{ij} d\delta_j}{h_{ij}^2 s_j} - \int_{-s_j}^{+s_j} \frac{\delta_j R'_{ij} d\delta_j}{[h'_{ij}]^2 s_j} \right\} \qquad (3)$$

Constants are defined as

$$R_{ij} = A + B\delta_j + \delta_i = A' + B\delta_j$$

where $A = y_{ij} \cos \phi_i + z_{ij} \sin \phi_i$

$A' = A + \delta_i$

$B = -\cos \phi_j \cos \phi_i - \sin \phi_j \sin \phi_i = -\cos(\phi_j - \phi_i)$

$$R'_{ij} = D + E\delta_j + \delta_i = D' + E\delta_j$$

where $D = y'_{ij} \cos \phi_i + z'_{ij} \sin \phi_i$

$D' = D + \delta_j$

$E = \cos \phi_j \cos \phi_i - \sin \phi_j \sin \phi_i = \cos(\phi_j + \phi_i)$

$$h_{ij}^2 = \delta_j^2 + (F + 2B\delta_i)\delta_j + (G + 2A\delta_i + \delta_i^2)$$

$$= \delta_j^2 + F'\delta_j + G'$$

where $F = -2(y_{ij} \cos \phi_j + z_{ij} \sin \phi_j)$

$F' = F + 2B\delta_i$

$G = z_{ij}^2 + y_{ij}^2$

$G' = G + 2A\delta_i + \delta_i^2$

and

$$(h'_{ij})^2 = \delta_j^2 + (J + 2E\delta_i)\delta_j + (K + 2D\delta_i + \delta_i^2)$$

$$= \delta_j^2 + J'\delta_j + K'$$

where $J = 2(y'_{ij} \cos \phi_j - z'_{ij} \sin \phi_j)$

$J' = J + 2E\delta_i$

$K = (z'_{ij})^2 + (y'_{ij})^2$

$K' = K + 2D\delta_i + \delta_i^2$

The normal wash is now written as

$$w_{n,j}(\delta_i) = \frac{\gamma_{j+1} + \gamma_j}{2} (A_{1_{ij}} + A_{2_{ij}}) + \frac{\gamma_{j+1} - \gamma_j}{2} (A_{3_{ij}} + A_{4_{ij}}) \qquad (4)$$

where

$$A_{1_{ij}} = \frac{1}{2\pi} \int_{-s_j}^{+s_j} \frac{A' + B\delta_j}{\delta_j^2 + F'\delta_j + G'} d\delta_j$$

$$A_{2_{ij}} = -\frac{1}{2\pi} \int_{-s_j}^{+s_j} \frac{D' + E\delta_j}{\delta_j^2 + J'\delta_j + K'} d\delta_j$$

$$A_{3_{ij}} = \frac{1}{2\pi s_j} \int_{-s_j}^{+s_j} \frac{A'\delta_j + B\delta_j^2}{\delta_j^2 + F'\delta_j + G'} d\delta_j$$

and

$$A_{4_{ij}} = -\frac{1}{2\pi s_j} \int_{-s_j}^{+s_j} \frac{D'\delta_j + E\delta_j^2}{\delta_j^2 + J'\delta_j + K'} d\delta_j$$

The above integrals contain constants, none of which contain δ_j. They can be integrated analytically to give

$$A_{1_{ij}} = \frac{1}{2\pi} \left\{ \left(A' - \frac{BF'}{2} \right) P + \frac{B}{2} \left(\ell n | s_j^2 + F's_j + G' | \right. \right.$$

$$\left. \left. - \ell n | s_j^2 - F's_j + G' | \right) \right\}$$

where

$$P = \frac{2}{\sqrt{4G' - F'^2}} \left\{ \tan^{-1}\left[\frac{F' + 2s_j}{(4G' - F'^2)^{1/2}} \right] - \tan^{-1}\left[\frac{F' - 2s_j}{(4G' - F'^2)^{1/2}} \right] \right\}$$

for

$$4G' - F'^2 \neq 0.$$

If $4G' - F'^2 = 0$, then $P = \frac{2}{F' - 2s_j} - \frac{2}{F' + 2s_j}$.

Next,

$$A_{2_{ij}} = \frac{-1}{2\pi} \left\{ \left(D' - \frac{J'E}{2} \right) Q + \frac{E}{2} \left(\ell n \left| s_j^2 + J's_j + K' \right| - \ell n \left| s_j^2 - J's_j + K' \right| \right) \right\}$$

where

$$Q = \frac{2}{\sqrt{(4K' - J'^2)}} \left\{ \tan^{-1}\left[\frac{J' + 2s_j}{(4K' - J'^2)^{1/2}} \right] - \tan^{-1}\left[\frac{J' - 2s_j}{(4K' - J'^2)^{1/2}} \right] \right\}$$

for

$$4K' - J'^2 \neq 0.$$

If $4K' - J'^2 = 0$, then $Q = \frac{2}{J' - 2s_j} - \frac{2}{J' + 2s_j}$.

Also,

$$A_{3_{ij}} = \frac{1}{2\pi s_j} \left\{ \left(\frac{-A'F' + BF'^2 - 2BG'}{2} \right) P + 2Bs_j + \left(\frac{A' - BF'}{2} \right) \left(\ell n \left| s_j^2 + F's_j + G' \right| - \ell n \left| s_j^2 - F's_j + G' \right| \right) \right\}$$

and

$$A_{4_{ij}} = \frac{-1}{2\pi s_j}\left\{\left(\frac{-D'J' + EJ'^2 - 2EK'}{2}\right)Q + 2Es_j + \left(\frac{D' - J'E}{2}\right)\left(\ell n\left|s_j^2 + J's_j + K'\right| - \ell n\left|s_j^2 - J's_j + K'\right|\right)\right\}$$

Note that

$$\sqrt{4G' - F'^2} = \left|R + T\delta_i\right|$$

where

$$R = 2(y_{ij}\sin\phi_j - z_{ij}\cos\phi_j)$$

$$T = 2\sin(\phi_j - \phi_i)$$

and

$$\sqrt{4K' - J'^2} = \left|U + W\delta_i\right|$$

where

$$U = 2(y'_{ij}\sin\phi_j + z'_{ij}\cos\phi_j)$$

$$W = 2\sin(\phi_j + \phi_i)$$

Now, written out in terms of the unprimed constants and the variable δ_i, the integrals appearing in equation (4) for the normal wash are

$$A_{1_{ij}} = \frac{1}{2\pi}\left\{\frac{\left(A - \frac{BF}{2} + (1 - B^2)\delta_i\right)}{\left|R + T\delta_i\right|}2\left(\tan^{-1}\left[\frac{F + 2s_j + 2B\delta_i}{\left|R + T\delta_i\right|}\right] - \tan^{-1}\left[\frac{F - 2s_j + 2B\delta_i}{\left|R + T\delta_i\right|}\right]\right)\right\} + \frac{B}{4\pi}\left\{\ell n\left|s_j^2 + Fs_j + G\right.\right.$$

$$+ 2(A + Bs_j)\delta_i + \delta_i^2| - \ell n|\delta_j^2 - Fs_j + G$$

$$+ 2(A - Bs_j)\delta_i + \delta_i^2|\Bigg\}$$

$$A_{2_{ij}} = \frac{-1}{2\pi}\Bigg\{\frac{\left(D - \frac{JE}{2} + (1 - E^2)\delta_i\right)}{|U + W\delta_i|} 2\left(\tan^{-1}\left[\frac{J + 2s_j + 2E\delta_i}{|U + W\delta_i|}\right]\right.$$

$$\left. - \tan^{-1}\left[\frac{J - 2s_j + 2E\delta_i}{|U + W\delta_i|}\right]\right) - \frac{E}{4\pi} \ell n|s_j^2 + Js_j + K$$

$$+ 2(D + Es_j)\delta_i + \delta_i^2| - \ell n|s_j^2 - Js_j + K$$

$$+ 2(D - Es_j)\delta_i + \delta_i^2|\Bigg\}$$

$$A_{3_{ij}} = \frac{1}{2\pi s_j}\Bigg\{\left[\frac{(BF^2 - AF - 2BG) + (-F - 6AB + 4B^2F)\delta_i + (4B^3 - 4B)\delta_i^2}{2}\right]$$

$$\frac{2}{|R + T\delta_i|}\left(\tan^{-1}\left[\frac{F + 2s_j + 2B\delta_i}{|R + T\delta_j|}\right] - \tan^{-1}\left[\frac{F - 2s_j + 2B\delta_i}{|R + T\delta_i|}\right]\right)\Bigg\}$$

$$+ \frac{B}{\pi} + \frac{1}{2\pi s_j}\left(\frac{A - BF + (1 - 2B^2)\delta_i}{2}\right)\Bigg\{\ell n|s_j^2 + Fs_j + G$$

$$+ 2(A + Bs_j)\delta_i + \delta_i^2| - \ell n|s_j^2 - Fs_j + G + 2(A - Bs_j)\delta_i + \delta_i^2|\Bigg\}$$

$$A_{4_{ij}} = \frac{-1}{2\pi s_j}\left\{\left[\frac{(EJ^2 - DJ - 2KE) + (-J - 6ED + 4E^2J)\delta_i + (4E^3 - 4E)\delta_i^2}{2}\right]\cdot\right.$$

$$\left.\cdot\frac{2}{|U + W\delta_i|}\left(\tan^{-1}\left[\frac{J + 2s_j + 2E\delta_i}{|U + W\delta_i|}\right] - \tan^{-1}\left[\frac{J - 2s_j + 2E\delta_i}{|U + W\delta_i|}\right]\right)\right\}$$

$$- \frac{E}{\pi} - \frac{1}{2\pi s_j}\left(\frac{D - EJ + (1 - 2E^2)\delta_i}{2}\right)\left\{\ell n\left|s_j^2 + Js_j + K\right.\right.$$

$$\left.\left. + 2(D + Es_j)\delta_i + \delta_i^2\right| - \ell n\left|s_j^2 - Js_j + K + 2(D - Es_j)\delta_i + \delta_i^2\right|\right\}$$

The four integrals above are now used to evaluate the induced drag on segment i due to the induced velocity at the wing due to segment j by integration of the product of bound circulation and normal wash. The induced drag for each linear segment is of the form

$$D_{ij} = \int_{-s_i}^{+s_i} \rho\, \Gamma(\delta_i)\left(\frac{1}{2} w_{n,j}(\delta_i)\right) d\delta_i$$

and thus, the corresponding drag coefficient is

$$C_{D,ij} = \frac{D_{ij}}{\frac{1}{2}\rho U^2 S_{ref}} = \frac{1}{S_{ref}} \int_{-s_i}^{+s_i} \frac{\Gamma(\delta_i)}{U}\left(\frac{w_{n,j}(\delta_i)}{U}\right) d\delta_i \qquad (5)$$

The bound circulation is found by the integration of the shed sheet strength from the tip to the desired location, such as

$$\Gamma(\delta_i) = \int_{tip}^{\delta_i} \gamma(\delta)d\delta = \Gamma_o(-s_i) + \int_{-s_i}^{\delta_i} \gamma(\delta_i)d\delta_i .$$

That is,

$$\Gamma(\delta_i) = \Gamma_o(-s_i) + \frac{s_i}{4}\left(\gamma_{i+1} + 3\gamma_i\right) + \left(\frac{\gamma_{i+1} + \gamma_i}{2}\right)\delta_i$$

$$+ \left(\frac{\gamma_{i+1} - \gamma_i}{2}\right)\frac{\delta_i^2}{2s_i}$$

where $\Gamma_o(-s_i)$ is the value of the bound circulation evaluated at $\delta_i = -s_i$. Specifically

$$\Gamma_o(-s_i) = \sum_{k=1}^{i-1}\int_{-s_k}^{s_k}\gamma(\delta_k)d\delta_k = \gamma_1 s_1 + \sum_{p=2}^{i-1}\gamma_p\left(s_p + s_{p-1}\right) + \gamma_i s_{i-1}$$

Then the induced drag coefficient on segment i due to segment j and its image is given by

$$C_{D,ij} = \frac{1}{S_{ref}}\int_{-s_i}^{+s_i}\left\{\frac{\Gamma_o(-s_i)}{U} + \frac{s_i}{4U}\left(\gamma_{i+1} + 3\gamma_i\right) + \left(\frac{\gamma_{i+1} + \gamma_i}{2U}\right)\delta_i\right.$$

$$\left. + \left(\frac{\gamma_{i+1} - \gamma_i}{2U}\right)\frac{\delta_i^2}{2s_i}\right\} \cdot \left\{\left(\frac{\gamma_{j+1} + \gamma_j}{2U}\right)\left(A_{1_{ij}} + A_{2_{ij}}\right)\right.$$

$$\left. + \left(\frac{\gamma_{j+1} - \gamma_j}{2U}\right)\left(A_{3_{ij}} + A_{4_{ij}}\right)\right\}d\delta_i \qquad (6)$$

Define

$$G_i = \frac{\Gamma_o(-s_i)}{U} + \frac{s_i}{4U}\left(\gamma_{i+1} + 3\gamma_i\right)$$

$$\bar{G}_i = \frac{\gamma_{i+1} + \gamma_i}{2U}; \quad \bar{G}_j = \frac{\gamma_{j+1} + \gamma_j}{2U}$$

$$\hat{G}_i = \frac{\gamma_{i+1} - \gamma_i}{2U}; \quad \hat{G}_j = \frac{\gamma_{j+1} - \gamma_j}{2U}$$

so that

$$C_{D,ij} = \frac{1}{S_{ref}} \left(G_i \bar{G}_j I_{1_{i,j}} + G_i \hat{G}_j I_{2_{i,j}} + \bar{G}_i \bar{G}_j I_{3_{i,j}} + \bar{G}_i \hat{G}_j I_{4_{i,j}} \right.$$

$$\left. + \hat{G}_i \bar{G}_j I_{5_{i,j}} + \hat{G}_i \hat{G}_j I_{6_{i,j}} \right) \tag{7}$$

where

$$I_{1_{i,j}} = \int_{-s_i}^{+s_i} (A_{1_{ij}} + A_{2_{ij}}) d\delta_i$$

$$I_{2_{i,j}} = \int_{-s_i}^{+s_i} (A_{3_{ij}} + A_{4_{ij}}) d\delta_i$$

$$I_{3_{i,j}} = \int_{-s_i}^{+s_i} \delta_i (A_{1_{ij}} + A_{2_{ij}}) d\delta_i$$

$$I_{4_{i,j}} = \int_{-s_i}^{+s_i} \delta_i (A_{3_{ij}} + A_{4_{ij}}) d\delta_i$$

$$I_{5_{i,j}} = \int_{-s_i}^{+s_i} \delta_i^2 \frac{(A_{1_{ij}} + A_{2_{ij}})}{2s_i} d\delta_i$$

$$I_{6_{i,j}} = \int_{-s_i}^{+s_i} \delta_i^2 \frac{(A_{3_{ij}} + A_{4_{ij}})}{2s_i} d\delta_i$$

These integrals with respect to δ_i are evaluated analytically using the MACSYMA symbolic manipulation language (ref. 12) as detailed in the Appendix. The following integrals require special consideration:

1. Integrals of the type

$$\int_{-s_i}^{+s_i} \delta_i^n \, \ell n \left| \delta_i^2 + E\delta_i + D \right| d\delta_i \qquad n = 0,1,2,3$$

are evaluated exactly except where a logarithmic singularity occurs, i.e., at the endpoint. There, the singularity is omitted from the range of integration. An analytical justification for the omission of such singularities has not yet been found. Instead, numerical studies have indicated that the omitted range can be varied from $(10^{-7})(s_i)$ to $(10^{-3})(s_i)$ and still not affect the solutions for bound circulation or induced drag to four significant figures. This therefore provides some numerical justification for the restricted range of integration.

2. Integrals of the type

$$\int_{-s_i}^{+s_i} \frac{\delta_i^n}{|R + T\delta_i|} \tan^{-1}\left\{\frac{c + 2B\delta_i}{|R + T\delta_i|}\right\} d\delta_i \qquad n = 0,1,2,3,4$$

are not generally integrable analytically; hence, they have been replaced by approximate integrals of the type

$$\int_{-s_i}^{+s_i} \frac{\delta_i^n(K_1\delta_i^2 + K_2\delta_i + K_3)}{|R + T\delta_i|} d\delta_i$$

which are then integrable analytically. The constants K_1, K_2, K_3, are chosen so the quadratic exactly equals the original inverse tangent function at $\delta_i = \pm s_i$ and zero. When $T = 0$ and $R \neq 0$, the original integral is integrated exactly. If both R and T equal zero, the remaining finite integral is of the form

$$\int_{-s_i}^{+s_i} \frac{-\delta_i^n}{c + 2B\delta_i} d\delta_i$$

which can also be integrated analytically. For these three types of integrals, the denominator is checked for singular behavior. If singularities are found to occur, they are excluded from the range of integration. Again, numerical studies have shown that this does not affect the solutions for Γ or induced drag. Such singularities are found to occur only at the wake segment endpoints and only when considering the velocity induced by one wake segment on an adjacent segment.

OPTIMIZATION

Using Munk's criterion (ref. 7) which states that

$$\frac{w_n}{\cos \phi} = w_o = \text{constant}, \tag{8}$$

a system of N_T linear equations is developed for the unknown shed sheet strengths, by equating the normal wash at each segment center to $\cos \phi$ on that segment. That is, following the techniques of references 4 and 13,

$$\cos \phi_i = \frac{1}{w_o} \sum_{j=1}^{N_T} \left\{ \left(\frac{\gamma_{j+1} + \gamma_j}{2} \right) \left(A_{1_{ij}} + A_{2_{ij}} \right) + \left(\frac{\gamma_{j+1} - \gamma_j}{2} \right) \left(A_{3_{ij}} + A_{4_{ij}} \right) \right\}$$

In the present formulation it has been assumed that the shed sheet strength on the wake centerline, γ_{N_T+1} equals zero. The resulting shed sheet strengths are scaled by the constant w_o. The ratio of w_o to the free stream speed is calculated from an evaluation of the lift coefficient. That is,

$$\frac{C_L}{2} = \frac{4}{S_{ref}} \left\{ \frac{1}{3} \sum_{i=1}^{N_T} \left(\cos \phi_i s_i^2 \left(\frac{\gamma_{i+1}}{w_o} + \frac{2\gamma_i}{w_o} \right) \right) + \sum_{i=1}^{N_T} \left(\cos \phi_i s_i \frac{\Gamma_o(-s_i)}{w_o} \right) \right\} \frac{w_o}{U} .$$

Once the optimum shed sheet strengths are found, the drag is calculated directly as described in the previous section. A drag efficiency factor is found, defined as the ratio of $(C_L^2/\pi A)$ for a planar wing of equal span to the calculated induced drag for the nonplanar configuration.

An alternative optimization technique which has been developed is to solve directly for the shed sheet strengths by writing the drag coefficient explicitly in terms of the unknown γ's, as in the previous section, and finding expressions for the derivatives of C_D with respect to the unknown scale factors. With

$$C_D = 2 \sum_{i=1}^{N_T} \sum_{j=1}^{N_T} C_{D,ij}$$

where as in equation (7)

$$C_{D,ij} = \frac{1}{S_{ref}} \left\{ G_i \bar{G}_j I_{1_{i,j}} + G_i \hat{G}_j I_{2_{i,j}} + \bar{G}_i \bar{G}_j I_{3_{i,j}} + \bar{G}_i \hat{G}_j I_{4_{i,j}} + \hat{G}_i \bar{G}_j I_{5_{i,j}} + \hat{G}_i \hat{G}_j I_{6_{i,j}} \right\}$$

it is necessary to calculate terms

$$\frac{\partial C_D}{\partial \gamma_p} \quad \text{for} \quad p = 1, \ldots\ldots, N_T$$

The following terms must be considered:

$$\frac{\partial \left\{ C_{D,ij} \right\}_{j=p}}{\partial \left\{ \frac{\gamma}{U} \right\}_p} = \frac{1}{S_{ref}} \left[\frac{G_i}{2} \left(I_{1_{i,p}} - I_{2_{i,p}} \right) + \frac{\bar{G}_i}{2} \left(I_{3_{i,p}} - I_{4_{i,p}} \right) + \frac{\hat{G}_i}{2} \left(I_{5_{i,p}} - I_{6_{i,p}} \right) \right]$$

$$\frac{\partial \left\{ C_{D,ij} \right\}_{j=p-1}}{\partial \left\{ \frac{\gamma}{U} \right\}_p} = \frac{1}{S_{ref}} \left[\frac{G_i}{2} \left(I_{1_{i,p-1}} + I_{2_{i,p-1}} \right) + \frac{\bar{G}_i}{2} \left(I_{3_{i,p-1}} + I_{4_{i,p-1}} \right) + \frac{\hat{G}_i}{2} \left(I_{5_{i,p-1}} + I_{6_{i,p-1}} \right) \right]$$

$$\frac{\partial \left\{ C_{D,ij} \right\}_{i=p}}{\partial \left\{ \frac{\gamma}{U} \right\}_p} = \frac{1}{S_{ref}} \left[\left(s_{p-1} + \frac{3s_p}{4} \right) \left(\bar{G}_j I_{1_{p,j}} + \hat{G}_j I_{2_{p,j}} \right) + \frac{1}{2} \left(\bar{G}_j \bar{I}_{3_{p,j}} + \hat{G}_j I_{4_{p,j}} - \bar{G}_j I_{5_{p,j}} - \hat{G}_j I_{6_{p,j}} \right) \right]$$

$$\frac{\partial \left\{C_{D,ij}\right\}_{i=p-1}}{\partial \left\{\frac{\gamma}{U}\right\}_p} = \frac{1}{S_{ref}} \left[\frac{s_{p-1}}{4} \left(\bar{G}_j I_{1_{p-1,j}} + \hat{G}_j I_{2_{p-1,j}} \right) + \frac{1}{2} \left(\bar{G}_j I_{3_{p-1,j}} + \hat{G}_j I_{4_{p-1,j}} + \bar{G}_j I_{5_{p-1,j}} + \hat{G}_j I_{6_{p-1,j}} \right) \right]$$

$$\frac{\partial \left\{C_{D,ij}\right\}_{i=p+m}}{\partial \left\{\frac{\gamma}{U}\right\}_p} = \frac{1}{S_{ref}} \left[\left(s_p + s_{p-1} \right) \left(\bar{G}_j I_{1_{p+m,j}} + \hat{G}_j I_{2_{p+m,j}} \right) \right], \quad m \geq 1$$

The lift coefficient constraint is satisfied through use of a Lagrange multiplier in the objective function, so that the function to be extremized becomes

$$2 \sum_{i=1}^{N_T} \sum_{j=1}^{N_T} C_{D,ij} + \lambda \left(\sum_{p=1}^{N_T} C_{L,p} \cdot \frac{\gamma_p}{U} - C_L \right)$$

Each equation in the optimization system can then be written as

$$A_{p,k} \gamma_k + \lambda C_{L,p} = 0, \quad p=1, \ldots N_T$$

where

$$A_{p,k} = \frac{2}{S_{ref}} \Bigg\{ \left(s_p + s_{p-1} \right) \left[\frac{1}{2} \sum_{m=1}^{N_T-p} \left(I_{1_{p+m,k}} - I_{2_{p+m,k}} + I_{1_{p+m,k-1}} + I_{2_{p+m,k-1}} \right) \right]$$

$$+ \frac{1}{2} \left(s_{p-1} + \frac{3}{4} s_p \right) \left(I_{1_{p,k}} + I_{1_{p,k-1}} - I_{2_{p,k}} + I_{2_{p,k-1}} \right)$$

$$+ \frac{1}{4} \Big\{ I_{3_{p,k}} + I_{3_{p,k-1}} - I_{4_{p,k}} + I_{4_{p,k-1}} - I_{5_{p,k}}$$

$$- I5_{p,k-1} + I6_{p,k} - I6_{p,k-1} \Bigg\}$$

$$+ \frac{s_{p-1}}{8} \left(I1_{p-1,k} + I1_{p-1,k-1} - I2_{p-1,k} + I2_{p-1,k-1} \right)$$

$$+ \frac{1}{4} \Big\{ I3_{p-1,k} + I3_{p-1,k-1} - I4_{p-1,k} + I4_{p-1,k-1} + I5_{p-1,k}$$

$$+ I5_{p-1,k-1} - I6_{p-1,k} + I6_{p-1,k-1} \Big\}$$

$$+ \frac{1}{4} \Big\{ I3_{k,p} + I3_{k,p-1} - I4_{k,p} + I4_{k,p-1} - I5_{k,p} - I5_{k,p-1} + I6_{k,p} - I6_{k,p-1} \Big\}$$

$$+ \frac{1}{4} \Big\{ I3_{k-1,p} + I3_{k-1,p-1} - I4_{k-1,p} + I4_{k-1,p-1} + I5_{k-1,p} + I5_{k-1,p-1}$$

$$- I6_{k-1,p} + I6_{k-1,p-1} \Big\}$$

$$+ \frac{s_{k-1}}{8} \left(I1_{k-1,p} + I1_{k-1,p-1} - I2_{k-1,p} + I2_{k-1,p-1} \right)$$

$$+ \frac{1}{2} \left(s_{k-1} + \frac{3}{4} s_k \right) \left(I1_{k,p} + I1_{k,p-1} - I2_{k,p} + I2_{k,p-1} \right)$$

$$+ \frac{1}{2} \left(s_k + s_{k-1} \right) \sum_{m=1}^{N_T-k} \left(I1_{k+m,p} + I1_{k+m,p-1} - I2_{k+m,p} + I2_{k+m,p-1} \right) \Bigg\}$$

And, since

$$C_L = \frac{8}{S_{ref}} \left\{ \frac{1}{3} \sum_{i=1}^{N_T} \cos \phi_i s_i^2 \left(\frac{\gamma_{i+1}}{U} + \frac{2\gamma_i}{U} \right) + \sum_{i=1}^{N_T} \cos \phi_i s_i \frac{\Gamma_o}{U} \left(-s_i \right) \right\}$$

then

$$\frac{\partial\left\{C_L\right\}}{\partial\left(\frac{\gamma_p}{U}\right)} = C_{L,p} = \frac{8}{S_{ref}}\left\{\frac{2}{3}\cos\phi_p s_p^2 + \frac{1}{3}\cos\phi_{p-1}s_{p-1}^2\right\}$$

$$+ \frac{8}{S_{ref}}\left\{\sum_{m=1}^{N_T-p}\left(\cos\phi_{p+m}s_{p+m}\right)\left(s_p + s_{p-1}\right) + \cos\phi_p s_p s_{p-1}\right\}$$

The $(N_T + 1)^{th}$ equation satisfies the lift coefficient constraint:

$$\sum_{p=1}^{N_T}\left\{C_{L,p}\cdot\ \frac{\gamma_p}{U}\right\} - C_L = 0$$

RESULTS AND DISCUSSIONS

The theoretical development has been implemented in an FORTRAN computer program which is operational on a CDC Cyber 173 machine, but it is not currently documented or available to outside users. A measure of the convergence, accuracy, and effect of segment spacing for the two optimization procedures is shown in figure 2. The induced drag coefficient calculated from direct integration of the drag expression obtained from the shed sheet strength values is compared with the exact result for a planar wing. Results are shown in terms of an efficiency factor, k, which is defined by Cone (ref. 9) and Lundry (ref. 10) as

$$k = \frac{C_D \text{ exact planar wing}}{C_D \text{ calculated}}$$

It is seen (note the stretched scale) that for both optimization techniques, k rapidly approaches the desired value, 1.0, as the number of wake segments

increases. Induced drag efficiencies for the direct optimization technique are very close to those calculated using Munk's criterion. However, as seen in figure 3 for $N_T = 10$, there are slight differences in the shed sheet strengths near the wing tip which are especially noticeable for equally spaced wake segments. Results similar to those shown in figure 3 indicate that the behavior of solutions for $N_T = 25$ and 50 is similar to those for $N_T = 10$, except the γ values lie closer to the exact distribution. Note the dramatic improvement in the representation of the wake vorticity distribution that is achieved using cosine spacing of the wake segments. Since the two optimization techniques yield nearly identical results, the remaining comparisons of the current theory with previous work will display only the Munk criterion optimization results.

In figure 4 induced drag efficiency factors for a planar wing computed using the current theory are compared with similar results obtained using a discrete trailing vortex Trefftz plane drag optimization program developed by J. R. Tulinius, B. B. Gloss, and J. L. Thomas of the NASA Langley Research Center using the method of reference 14. The error in the present theory with $N_T = 10$ is 1 percent with equal spacing and 0.2 percent with cosine spacing. This error using equally spaced segments is seen to be approximately one-fourth to one-fifth the error in efficiency obtained using the technique of reference 14. Errors for the current theory using cosine spacing are five times smaller still. The bound circulation values calculated from the Munk criterion solution shed sheet strengths are compared with the exact elliptical distribution in figure 5 for $N_T = 10$ and 25. Errors in calculated Γ values are even smaller than any errors in γ.

Optimization results for nonplanar configurations are compared with exact solutions in figures 6, 7, 8, and 9. The k values for a nonplanar configuration composed of a flat wing with a vertical endplate are compared in figure 6 with those of Lundry and Lissaman (ref. 11). Results shown are from the downwash criterion optimization using $N_T = 30$, with the wake segments distributed nearly uniformly on the wing and endplate and $\phi = 89.9°$, and with cosine spaced segments and $\phi = 89.7°$. The endplate is only approximately vertical to avoid numerical difficulties at $\phi = 90°$. The k values are somewhat sensitive to the value of ϕ chosen, but at $\phi = 89.7°$ with 30 cosine spaced wake segments the accuracy of the present method is comparable to the

method of reference 14 using 100 equally spaced discrete vortices. Note the relatively large error at $\ell/s = 0.2$ for equal spacing.

In figure 7 the induced drag efficiency for a wing with constant nonzero dihedral ($\phi = 30°$) outboard of $\eta = 0.5$ is shown compared with the solution given by Lundry (ref. 10) at $\ell/s = 0$. Results also compare well with a solution given by Mangler (ref. 8). The current code cannot handle vertical fences ($\ell/s > 0$), but this capability could be added.

In figures 8 and 9 results for wings having spanwise camber such that the wake is an arc of a circle are compared with an exact solution for such wakes by Cone (ref. 9). All results are from the constant downwash formulation of the optimization. Figure 8 compares the induced drag efficiency, and figure 9 shows the bound circulation values. The parameter β is defined as

$$\beta = \frac{d}{b/2}$$

where d is the maximum vertical dimension due to the spanwise camber. A value of $\beta = 0$ corresponds to a flat wing, and $\beta = 1.0$ corresponds to a semicircular wing. Present results with $N_T = 25$ again display an accuracy comparable to that of the method of reference 14 with 100 discrete wake trailing vortices.

CONCLUSIONS

The current drag optimization techniques assuming a piecewise linearly varying wake vortex sheet strength agree well with each other and with available exact solutions for a variety of Trefftz plane wake shapes. Agreement for overall drag efficiency factors and bound circulation distributions is generally better than one percent for on the order of 25 to 50 wake segments. Computational times generally run from 1 to 10 seconds on a CDC Cyber 173 machine. Accuracy of the present theory is approximately four to five times better than a discrete trailing vortex theory using the same number of unknowns and equal spacing of the wake segments. Cosine wake segment spacing leads to a further increase in accuracy.

APPENDIX

EVALUATION OF INTEGRALS IN DRAG EXPRESSION

The following is a compilation of the integrals utilized in the evaluation of the drag expression [eq. (6)] in the text, which are not generally available in integral tables. They have been evaluated through use of the MACSYMA symbolic manipulation language (ref. 12), and are repeated here for completeness.

1. Integrals of the type $\int_{-s}^{s} \delta^n \ln(\delta^2 + E\delta + D)d\delta$ depend upon whether $E^2 - 4D$ is positive, negative or zero. Results for all three are given, starting with $E^2 - 4D > 0$. For this case

$$\int_{-s}^{s} \ln(\delta^2 + E\delta + D)d\delta = \frac{-1}{2}\sqrt{E^2 - 4D}\,\ln\left(\frac{2s - \sqrt{E^2 - 4D} + E}{2s + \sqrt{E^2 - 4D} + E}\right)$$

$$+ s\,\ln\left[(s^2 + Es + D)(s^2 - Es + D)\right] - 4s$$

$$+ \frac{E}{2} \cdot \ln\frac{s^2 + Es + D}{s^2 - Es + D} + \frac{1}{2}\sqrt{E^2 - 4D}\,\ln\left(\frac{-2s - \sqrt{E^2 - 4D} + E}{-2s + \sqrt{E^2 - 4D} + E}\right)$$

$$\int_{-s}^{s} \delta\,\ln(\delta^2 + E\delta + D)d\delta = \frac{1}{4}E\sqrt{E^2 - 4D}\left\{\ln\left(\frac{2s - \sqrt{E^2 - 4D} + E}{2s + \sqrt{E^2 + 4D} + E}\right)\right.$$

$$\left. - \ln\left(\frac{-2s - \sqrt{E^2 - 4D} + E}{-2s + \sqrt{E^2 - 4D} + E}\right)\right\} + \frac{E^2 - 2D}{4}\left\{\ln\left(\frac{(s^2 - Es + D)}{(s^2 + Es + D)}\right)\right\}$$

$$+ \frac{s^2}{2}\ln\left(\frac{s^2 + Es + D}{s^2 - Es + D}\right) + Es$$

$$\int_{-s}^{s} \delta^2 \ln(\delta^2 + E\delta + D)d\delta = \frac{1}{6}\frac{E^4 - 5DE^2 + 4D^2}{\sqrt{E^2 - 4D}} \left\{ - \ln\left(\frac{2s - \sqrt{E^2 - 4D} + E}{2s + \sqrt{E^2 - 4D} + E}\right) \right.$$

$$\left. + \ln\left(\frac{-2s - \sqrt{E^2 - 4D} + E}{-2s + \sqrt{E^2 - 4D} + E}\right) \right\}$$

$$+ \frac{s^3}{3} \cdot \left[\ln(s^2 + Es + D)(s^2 - Es + D) \right]$$

$$+ \frac{1}{6} \cdot (E^3 - 3DE) \ln\left(\frac{s^2 + Es + D}{s^2 - Es + D}\right)$$

$$- \frac{4s^3}{9} - \frac{2}{3}(E^2 - 2D)s$$

$$\int_{-s}^{s} \delta^3 \ln(\delta^2 + E\delta + D)d\delta = \frac{(E^5 - 6DE^3 + 8D^2E)}{8\sqrt{E^2 - 4D}} \left\{ \ln\left(\frac{2s - \sqrt{E^2 - 4D} + E}{2s + \sqrt{E^2 - 4D} + E}\right) \right.$$

$$\left. - \ln\left(\frac{-2s - \sqrt{E^2 - 4D} + E}{-2s + \sqrt{E^2 - 4D} + E}\right) \right\}$$

$$+ \frac{E^4 - 4DE^2 + 2D^2}{8} \ln\left(\frac{s^2 - Es + D}{s^2 + Es + D}\right)$$

$$+ \frac{s^4}{4} \ln\left(\frac{s^2 + Es + D}{s^2 - Es + D}\right) + \frac{Es^3}{6} - \frac{(3D + E^2)sE}{2}$$

For $E^2 - 4D = 0$,

$$\int_{-s}^{s} \ell n(\delta^2 + E\delta + D)d\delta = s\ \ell n\left[(s^2 + Es + D)(s^2 - Es + D)\right]$$

$$+ E\ \ell n\left(\frac{E + 2s}{E - 2s}\right) - 4s$$

$$\int_{-s}^{s} \delta\ \ell n(\delta^2 + E\delta + D)d\delta = \frac{s^2}{2}\ \ell n\left(\frac{s^2 + Es + D}{s^2 - Es + D}\right) + \frac{E^2 - 2D}{2} \cdot$$

$$\cdot\ \ell n\left(\frac{E - 2s}{E + 2s}\right) + Es$$

$$\int_{-s}^{s} \delta^2\ \ell n(\delta^2 + E\delta + D)d\delta = \frac{s^3}{3}\ \ell n\left[(s^2 + Es + D)(s^2 - Es + D)\right]$$

$$+ \frac{(E^4 - 5DE^2 + 4D^2)}{3}\left(\frac{1}{E + 2s} - \frac{1}{E - 2s}\right)$$

$$+ E\left(D - \frac{E^2}{3}\right)\ell n\left(\frac{E - 2s}{E + 2s}\right) - \frac{4s^3}{9} - \frac{2}{3}(E^2 - 2D)s$$

$$\int_{-s}^{s} \delta^3\ \ell n(\delta^2 + E\delta + D)d\delta = \frac{s^4}{4}\ \ell n\left(\frac{s^2 + Es + D}{s^2 - Es + D}\right) + \frac{E^4 - 4DE^2 + 2D^2}{4} \cdot$$

$$\cdot\ \ell n\left(\frac{E - 2s}{E + 2s}\right) + \left(\frac{E^5 - 6DE^3 + 8D^2E}{4}\right) \cdot$$

$$\cdot\left(\frac{1}{E - 2s} - \frac{1}{E + 2s}\right) + \frac{Es^3}{6} - \frac{Es}{2}\ (3D - E^2)$$

For $E^2 - 4D < 0$

$$\int_{-s}^{s} \ell n(s^2 + Es + D)\,ds = s\ell n(s^2 + Es + D)(s^2 - Es + D)$$

$$+ \frac{E}{2} \ell n\left(\frac{s^2 + Es + D}{s^2 - Es + D}\right) - 4s - \sqrt{4D - E^2} \cdot$$

$$\cdot \left(- \tan^{-1}\left(\frac{E - 2s}{\sqrt{4D - E^2}}\right) + \tan^{-1}\left(\frac{E + 2s}{\sqrt{4D - E^2}}\right)\right)$$

$$\int_{-s}^{s} s\ \ell n(s^2 + Es + D)\,ds = \frac{E^2 - 2D}{4} \ell n\left(\frac{s^2 - Es + D}{s^2 + Es + D}\right) + \frac{s^2}{2} \cdot$$

$$\cdot \ell n\left(\frac{s^2 + Es + D}{s^2 - Es + D}\right) + Es + \frac{E}{2}\sqrt{4D - E^2} \cdot$$

$$\cdot \left(\tan^{-1}\left(\frac{E - 2s}{\sqrt{4D - E^2}}\right) - \tan^{-1}\left(\frac{E + 2s}{\sqrt{4D - E^2}}\right)\right)$$

$$\int_{-s}^{s} s^2\ \ell n(s^2 + Es + D)\,ds = \frac{E^3 - 3DE}{6} \ell n\left(\frac{s^2 + Es + D}{s^2 - Es + D}\right) - \frac{4}{9} s^3$$

$$- \frac{2s}{3}(E^2 - 2D) + \frac{E^4 - 5DE^2 + 4D^2}{3\sqrt{4D - E^2}} \cdot$$

$$\cdot \left(\tan^{-1}\left(\frac{E - 2s}{\sqrt{4D - E^2}}\right) - \tan^{-1}\left(\frac{E + 2s}{\sqrt{4D - E^2}}\right)\right)$$

$$+ \frac{s^3}{3} \ell n\left[(s^2 + Es + D)(s^2 - Es + D)\right]$$

$$\int_{-s}^{s} \delta^3 \ln(\delta^2 + E\delta + D)\,d\delta = \frac{E^4 - 4DE^2 + 2D^2}{8} \ln\left(\frac{s^2 - Es + D}{s^2 + Es + D}\right)$$

$$+ \frac{s^4}{4} \ln\left(\frac{s^2 + Es + D}{s^2 - Es + D}\right)$$

$$+ \left(\frac{-E^5 + 6DE^3 - 8D^2E}{4\sqrt{4D - E^2}}\right)\left(\tan^{-1}\left(\frac{E - 2s}{\sqrt{4D - E^2}}\right)\right.$$

$$\left. - \tan^{-1}\left(\frac{E + 2s}{\sqrt{4D - E^2}}\right)\right) + \frac{Es^3}{6} - \frac{Es}{2}(3D - E^2)$$

2. Integrals of the type

$\int_{-s}^{s} \frac{\delta^n}{|R + T\delta|} \tan^{-1}\left(\frac{c + 2B\delta}{|R + T\delta|}\right) d\delta$ are in general replaced by approximate integrals

$\int_{-s}^{s} \frac{\delta^n(K_1\delta^2 + K_2\delta + K_3)}{|R + T\delta|} d\delta$, where the K_1, K_2, K_3 are chosen to force the quadratic approximation to the inverse tangent function through the exact integrand at s = -s, 0, +s. Hence, the integrals are evaluated as follows:

For n = o,

$$\int_{-s}^{s} \frac{K_1\delta^2 + K_2\delta + K_3}{|R + T\delta|} d\delta = \frac{(K_3T^2 - K_2RT + K_1R^2)}{T^3} \ln\left(\frac{|R + Ts|}{|R - Ts|}\right)$$

$$+ \frac{s}{T^2}(2K_2T - 2K_1R)$$

for n = 1,

$$\int_{-s}^{s} \frac{(K_1\delta^2 + K_2\delta + K_3)}{|R + T\delta|}\, d\delta = \frac{(K_3RT^2 - K_2R^2T + K_1R^3)}{T^4}\, \ell n\left(\frac{|R - Ts|}{|R + Ts|}\right)$$

$$+ \frac{s}{3T^3}(6K_3T^2 - 6K_2RT + 6K_1R^2) + \frac{2K_1}{3T}\, s^3$$

for n = 2,

$$\int_{-s}^{s} \delta^2 \frac{(K_1\delta^2 + K_2\delta + K^3)}{|R + T\delta|}\, d\delta = \frac{(K_3R^2T^2 - K_2R^3T + K_1R^4)}{T^5}\, \ell n\left(\frac{|R + Ts|}{|R - Ts|}\right)$$

$$+ \frac{s^3}{6T^2}(4K_2T - 4K_1R) + \frac{2s}{T^4} \cdot$$

$$\cdot\, (\, - K_3RT^2 + K_2R^2T - K_1R^3)$$

for n = 3,

$$\int_{-s}^{s} \delta^3 \frac{(K_1\delta^2 + K_2\delta + K_3)}{|R + T\delta|}\, d\delta = \frac{(K_3R^3T^2 - K_2R^4T + K_1R^5)}{T^6} \cdot$$

$$\cdot\, \ell n\left(\frac{|R - Ts|}{|R + Ts|}\right) + \frac{2s^5K_1}{5T}$$

$$+ \frac{s^3}{3T^3}\, (2K_3T^2 - 2K_2RT + 2K_1R^2)$$

$$+ \frac{2s}{T^5}\, (K_3T^2R^2 - K_2R^3T + K_1R^4)$$

for n = 4,

$$\int_{-s}^{s} \delta^4 \frac{(K\delta^2 + K_2\delta + K_3)}{|R + T\delta|}\, d\delta = \frac{(K_3R^4T^2 - K_2R^5T + K_1R^6)}{T^7} \cdot$$

$$\cdot \ell n\left(\frac{|R + Ts|}{|R - Ts|}\right) + 2\,\frac{(K_2T - K_1R)}{5T^2}\, s^5$$

$$+ 2\,\frac{(-K_3RT^2 + K_2R^2T - K_1R^3)}{3T^4} \cdot$$

$$\cdot \left(s^3 + \frac{3R^2s}{T^2}\right)$$

When T = 0 and R ≠ 0, the integrals are evaluated analytically at

n = 0,

$$\int_{-s}^{s} \frac{1}{|R|} \tan^{-1}\left(\frac{c + 2B\delta}{|R|}\right) d\delta = \frac{1}{4B} \ell n\left(\frac{4B^2s^2 - 4Bcs + R^2 + c^2}{4B^2s^2 + 4Bcs + R^2 + c^2}\right)$$

$$+ \frac{c}{2B|R|}\left(\tan^{-1}\left(\frac{c + 2Bs}{|R|}\right) - \tan^{-1}\left(\frac{c - 2Bs}{|R|}\right)\right)$$

$$+ \frac{s}{|R|}\left(\tan^{-1}\left(\frac{c + 2Bs}{|R|}\right) + \tan^{-1}\left(\frac{c - 2Bs}{|R|}\right)\right)$$

n = 1,

$$\int_{-s}^{s} \frac{\delta}{|R|} \tan^{-1}\left(\frac{c + 2B\delta}{|R|}\right) d\delta = \frac{c}{8B^2} \ell n \left(\frac{4B^2s^2 + 4Bcs + R^2 + c^2}{4B^2s^2 - 4Bcs + R^2 + c^2}\right) - \frac{s}{2B}$$

$$+ \frac{(R^2 - c^2)}{8B^2|R|} \left(\tan^{-1}\left(\frac{c + 2Bs}{|R|}\right)\right.$$

$$\left. - \tan^{-1}\left(\frac{c - 2Bs}{|R|}\right)\right) + \frac{s^2}{2|R|} \left(\tan^{-1}\left(\frac{c + 2Bs}{|R|}\right)\right.$$

$$\left. - \tan^{-1}\left(\frac{c - 2Bs}{|R|}\right)\right)$$

$n = 2,$

$$\int_{-s}^{s} \frac{\delta^2}{|R|} \tan^{-1}\left(\frac{c + 2B\delta}{|R|}\right) d\delta = \frac{s^3}{3|R|} \left(\tan^{-1}\left(\frac{c + 2Bs}{|R|}\right) + \tan^{-1}\left(\frac{c - 2Bs}{|R|}\right)\right)$$

$$+ \frac{cs}{3B^2} + \frac{3R^2c - c^3}{24B^3|R|} \left(\tan^{-1}\left(\frac{c - 2Bs}{|R|}\right)\right.$$

$$\left. - \tan^{-1}\left(\frac{c + 2Bs}{|R|}\right)\right) + \frac{R^2 - 3c^2}{48B^3} \cdot$$

$$\cdot \ell n \left(\frac{4B^2s^2 + 4Bcs + R^2 + c^2}{4B^2s^2 - 4Bcs + R^2 + c^2}\right)$$

n = 3,

$$\int_{-s}^{s} \frac{\delta^3}{|R|} \tan^{-1}\left(\frac{c + 2B\delta}{|R|}\right) d\delta = \frac{c(R^2 - c^2)}{32B^4} \ell n \left(\frac{4B^2s^2 - 4Bcs + R^2 + c^2}{4B^2s^2 + 4Bcs + R^2 + c^2}\right)$$

$$+ \frac{(R^4 - 6c^2R^2 + c^4)}{64B^4|R|} \left(\tan^{-1}\left(\frac{c - 2Bs}{|R|}\right)\right.$$

$$\left. - \tan^{-1}\left(\frac{c + 2Bs}{|R|}\right)\right) + \frac{s^4}{4|R|} \left(\tan^{-1}\left(\frac{c + 2Bs}{|R|}\right)\right.$$

$$\left. - \tan^{-1}\left(\frac{c - 2Bs}{|R|}\right)\right) - \frac{s^3}{12B} - \frac{(3c^2 - R^2)s}{16B^3}$$

n = 4,

$$\int_{-s}^{s} \frac{\delta^4}{|R|} \tan^{-1}\left(\frac{c + 2B\delta}{|R|}\right) d\delta = \frac{s^5}{5|R|} \left(\tan^{-1}\left(\frac{c + 2Bs}{|R|}\right) + \tan^{-1}\left(\frac{c - 2Bs}{|R|}\right)\right)$$

$$+ \frac{(5cR^4 - 10c^3R^2 + c^5)}{160B^5|R|} \left(\tan^{-1}\left(\frac{c + 2Bs}{|R|}\right)\right.$$

$$\left. - \tan^{-1}\left(\frac{c - 2Bs}{R}\right)\right) + \frac{cs^3}{15B^2}$$

$$+ \frac{R^4 - 10c^2R^2 + 5c^4}{320B^5} .$$

continued

$$\cdot \ln\left(\frac{4B^2s^2 - 4Bcs + R^2 + c^2}{4B^2s^2 + 4Bcs + R^2 + c^2}\right)$$

$$+ \frac{c^3 - cR^2}{10B^4} s$$

When both R and T = 0, integrals of the following forms are evaluated as:

n = 0,

$$-\int_{-s}^{s} \frac{d\delta}{c + 2B\delta} = -\frac{1}{2B} \ln\left(\frac{c + 2Bs}{c - 2Bs}\right)$$

n = 1,

$$-\int_{-s}^{s} \frac{\delta d\delta}{c + 2B\delta} = \frac{c}{4B^2} \ln\left(\frac{c + 2Bs}{c - 2Bs}\right) - \frac{s}{B}$$

n = 2,

$$-\int_{-s}^{s} \frac{\delta^2 d\delta}{c + 2B\delta} = -\frac{c^2}{8B^3} \ln\left(\frac{c + 2Bs}{c - 2Bs}\right) + \frac{cs}{2B^2}$$

n = 3,

$$-\int_{-s}^{s} \frac{\delta^3 d\delta}{c + 2B\delta} = \frac{c^3}{16B^4} \ln\left(\frac{c + 2Bs}{c - 2Bs}\right) - \frac{s^3}{3B} - \frac{c^2 s}{4B^3}$$

n = 4,

$$-\int_{-s}^{s} \frac{\delta^4 d\delta}{c + 2B\delta} = \frac{-c^4}{32B^5} \ln\left(\frac{c + 2Bs}{c - 2Bs}\right) + \frac{cs^3}{6B^2} + \frac{c^3 s}{8B^4}$$

REFERENCES

1. Lamar, John E.: A Vortex Lattice Method for the Mean Camber Shapes of Trimmed Noncoplanar Planforms with Minimum Vortex Drag. NASA TN D-8090, June 1976.

2. Feifel, W.M.: Optimization and Design of Three-Dimensional Aerodynamic Configurations of Arbitrary Shape by a Vortex-Lattice Method. NASA SP-405, proceedings of Vortex-Lattice Utilization Workshop held at Langley Research Center, Hampton, VA, May 17-18, 1976.

3. Ishimitsu, K.K.: Aerodynamic Design and Analysis of Winglets. AIAA paper 76-940, presented at AIAA Aircraft Systems and Technology Meeting, Dallas, Texas, September 27-29, 1976.

4. Loth, John L.; and Boyle, Robert E.: Optimum Loading on Nonplanar Wings at Miminum Induced Drag. Aerospace Engineering TR-19, West Virginia University, August 1969.

5. Goldhammer, M.I.: A Lifting Surface Theory for the Analysis of Nonplanar Lifting Systems. AIAA paper No. 76-16, presented at 14th Aerospace Sciences Meeting, Washington, D.C., January 26-28, 1976.

6. Clever, W.C.: Spanwise Variation of Potential Form Drag. NASA CR-145180, May 1977.

7. Munk, Max M.: The Minimum Induced Drag of Airfoils. NACA Report 121, 1921.

8. Mangler, W.: The lift Distribution of Wings with End Plates. NACA TM No. 856, 1938.

9. Cone, C.D., Jr.: The Theory of Induced Lift and Minimum Induced Drag for Nonplanar Lifting Systems. NASA Technical Report R-139, 1962.

10. Lundry, J.L.: A Numerical Solution for the Minimum Induced Drag, and the Corresponding Loading, of Nonplanar Wings. NASA CR-1218, 1968.

11. Lundry, J.L.; and Lissaman, P.B.S.: A Numerical Solution for the Minimum Induced Drag of Nonplanar Wings. J. Aircraft, Vol. 5, No. 1, 1968.

12. MACSYMA Reference Manual, Version 8. The Mathlab Group, Project MAC, Massachusetts Institute of Technology, November 1975.

13. Blackwell, J.A., Jr.: Numerical Method to Calculate the Induced Drag or Optimum Loading for Arbitrary Non-Planar Aircraft. NASA SP-405, proceedings of Vortex-Lattice Utilization Workshop held at Langley Research Center, Hampton, VA, May 17-18, 1976.

14. Tulinius, J.; Clever, W.; Niemann, A.; Dunn, K.; and Gaither, B.: Theoretical Prediction of Airplane Stability Derivatives at Subcritical Speeds. NASA CR-132681, 1975.

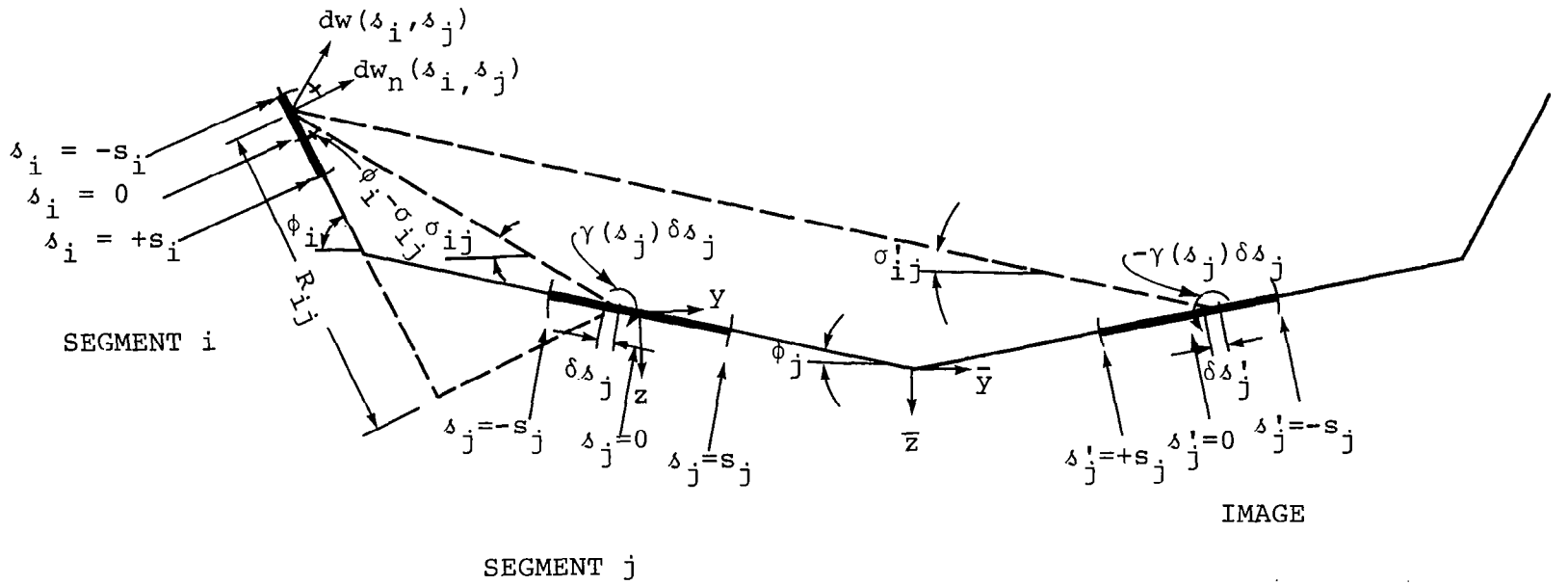

Figure 1. Trefftz plane geometry used in the present method.

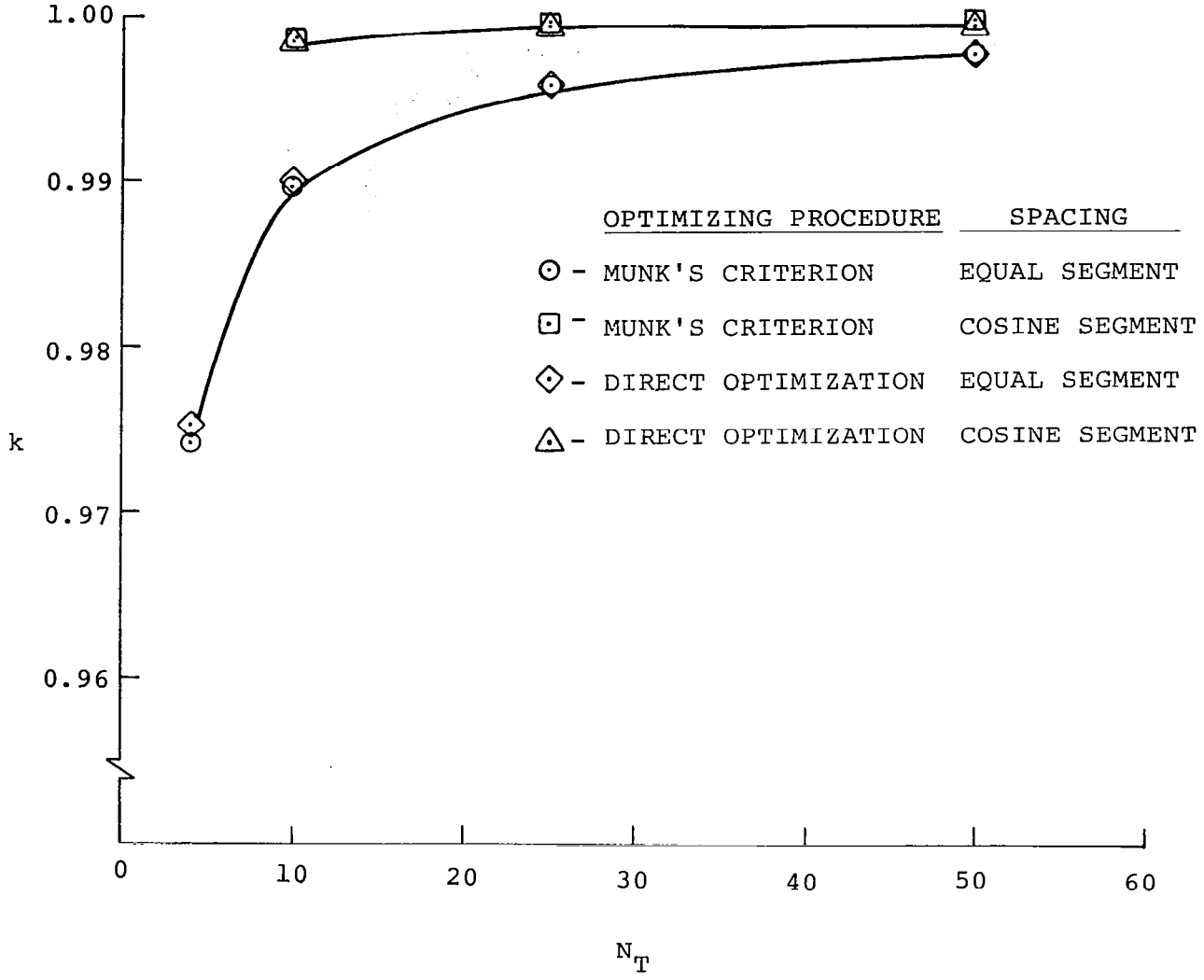

Figure 2. Effect of optimizing procedure and spacing on convergence of the induced drag efficiency for planar wings.

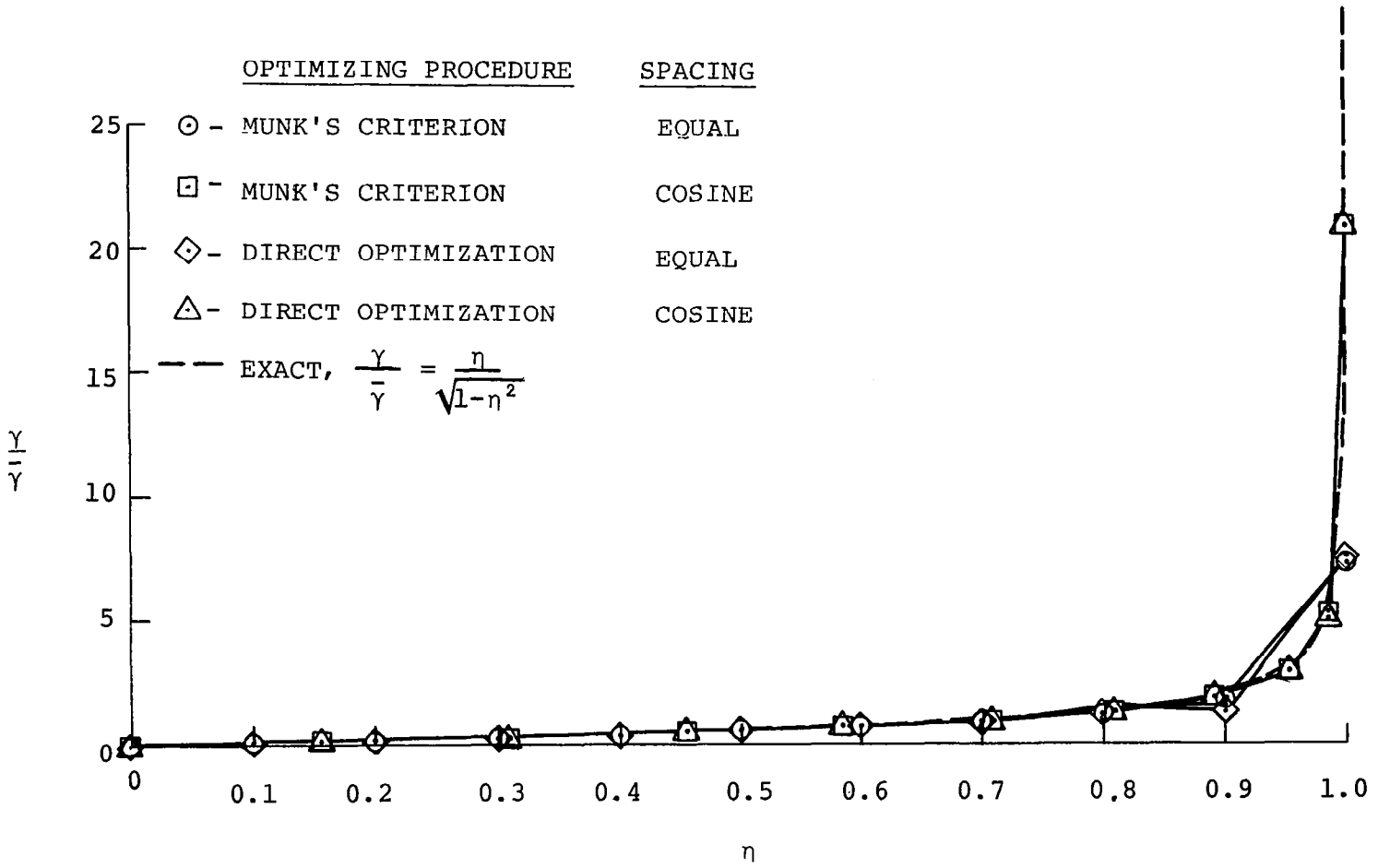

Figure 3. Effect of optimizing procedure and spacing on the wake strength for planar wings, $N_T = 10$.

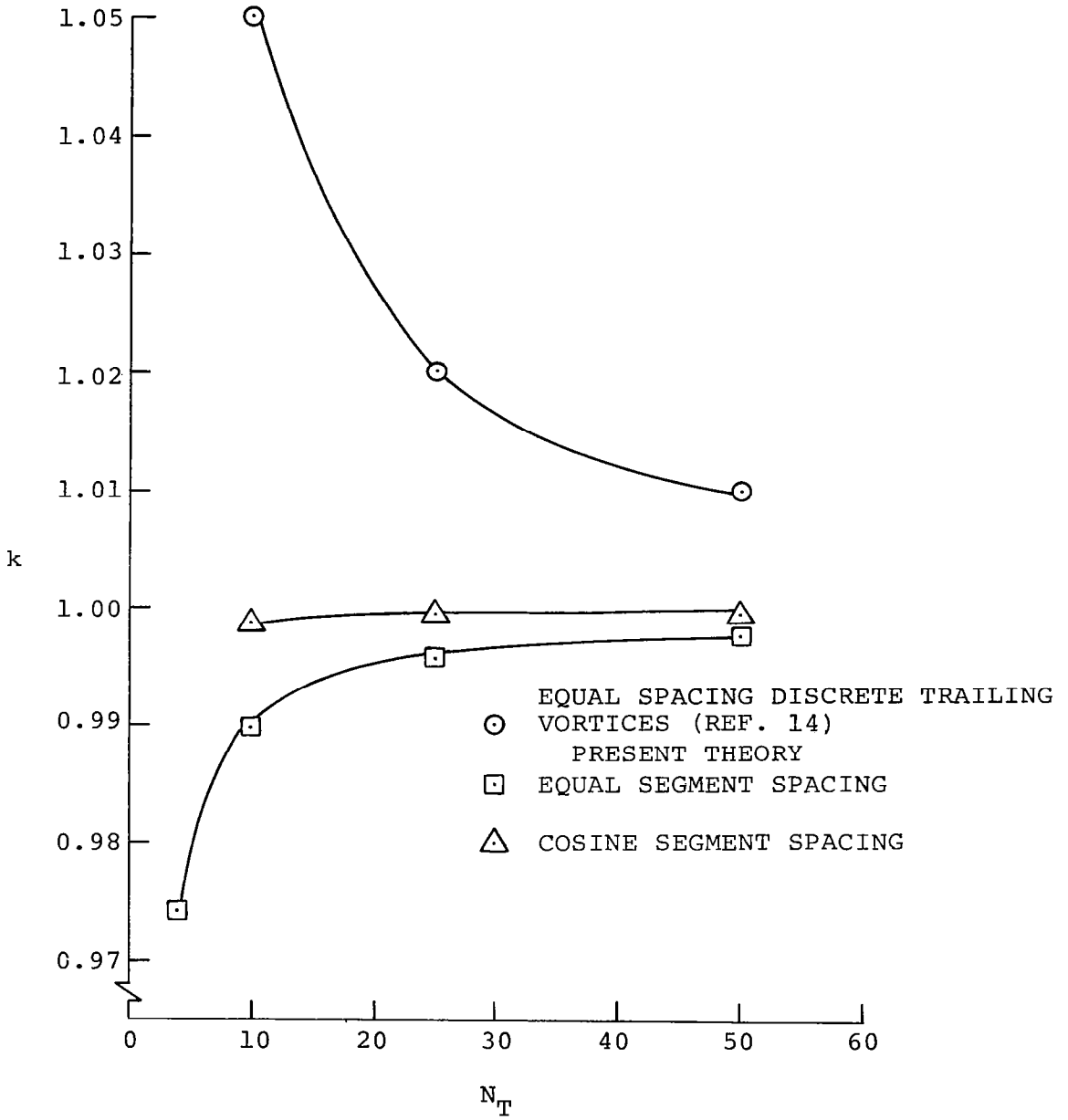

Figure 4. Convergence of induced drag optimization using Munk's criterion for planar wings.

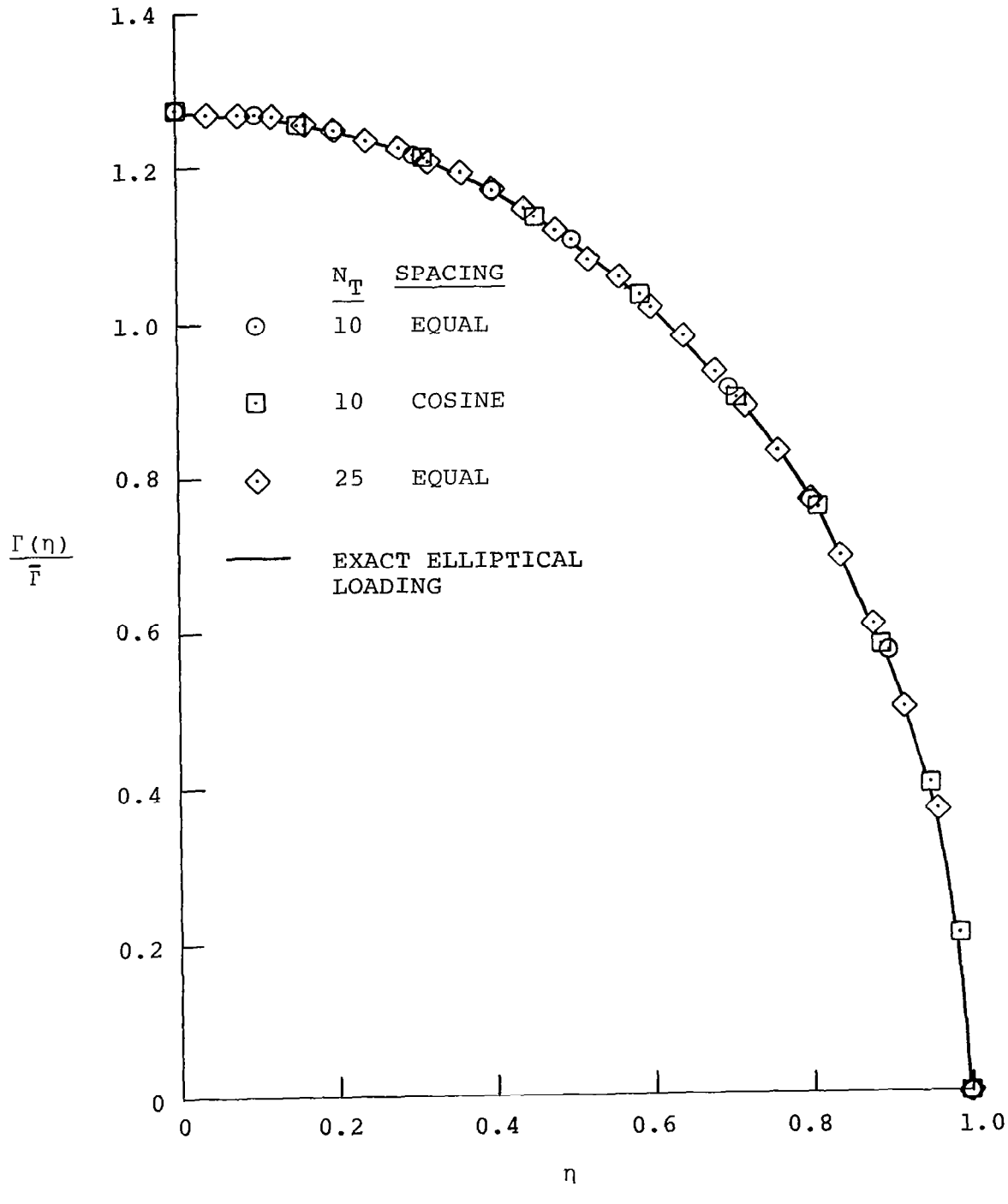

Figure 5. Effect of N_T and spacing on the bound circulations for planar wings using Munk's criterion.

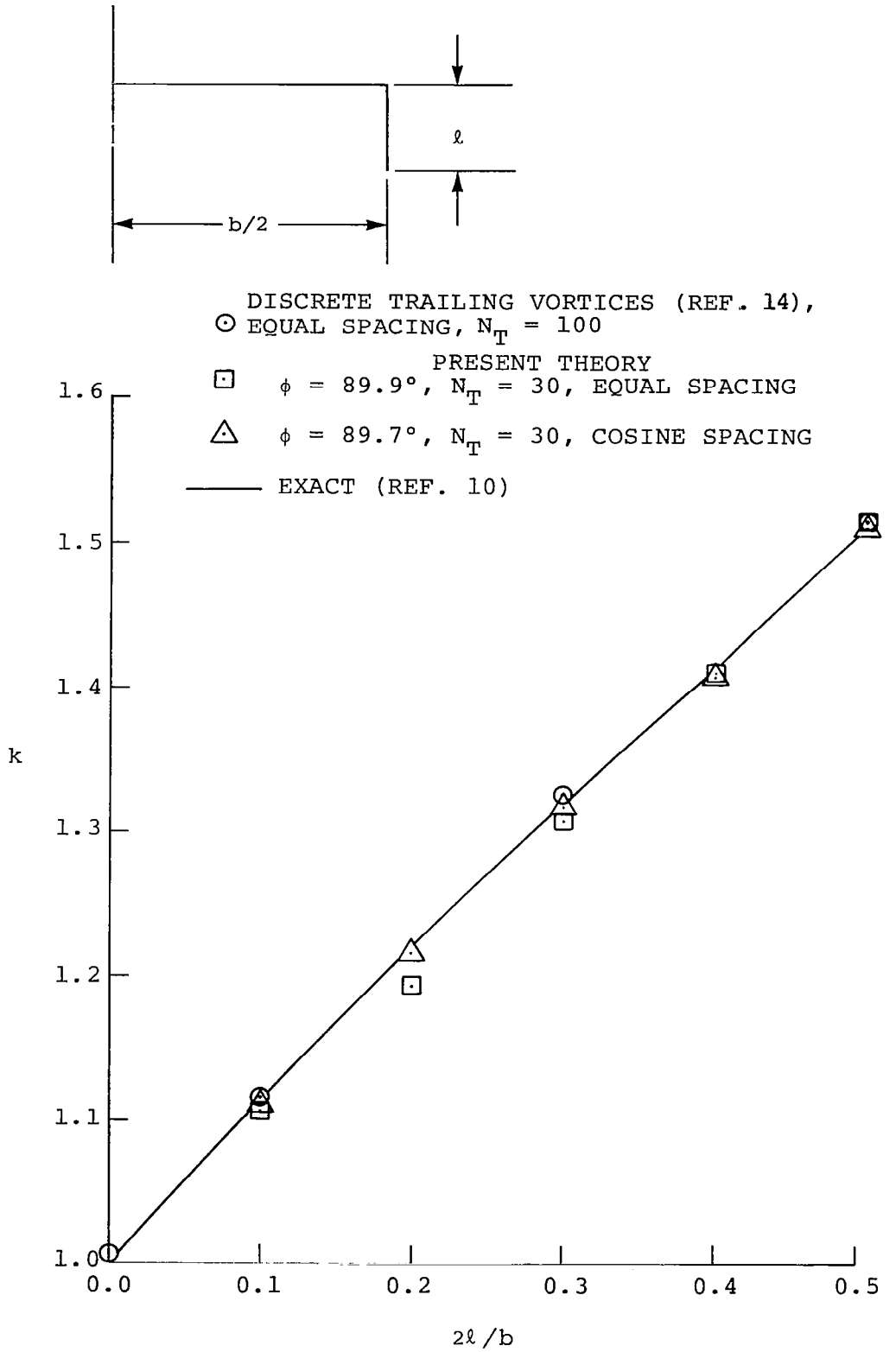

Figure 6. Induced drag efficiency for a wing with vertical endplates.

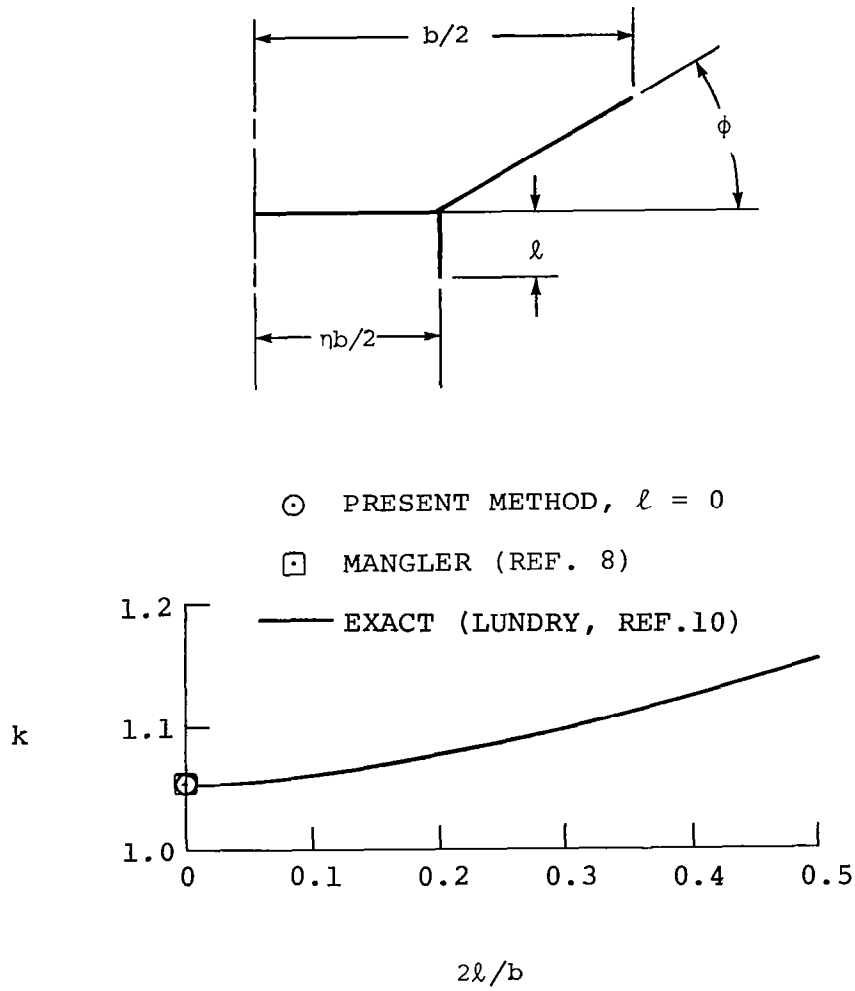

Figure 7. Induced drag efficiency for a wing with outboard dihedral, $\phi = 30°$, $\eta = 0.5$.

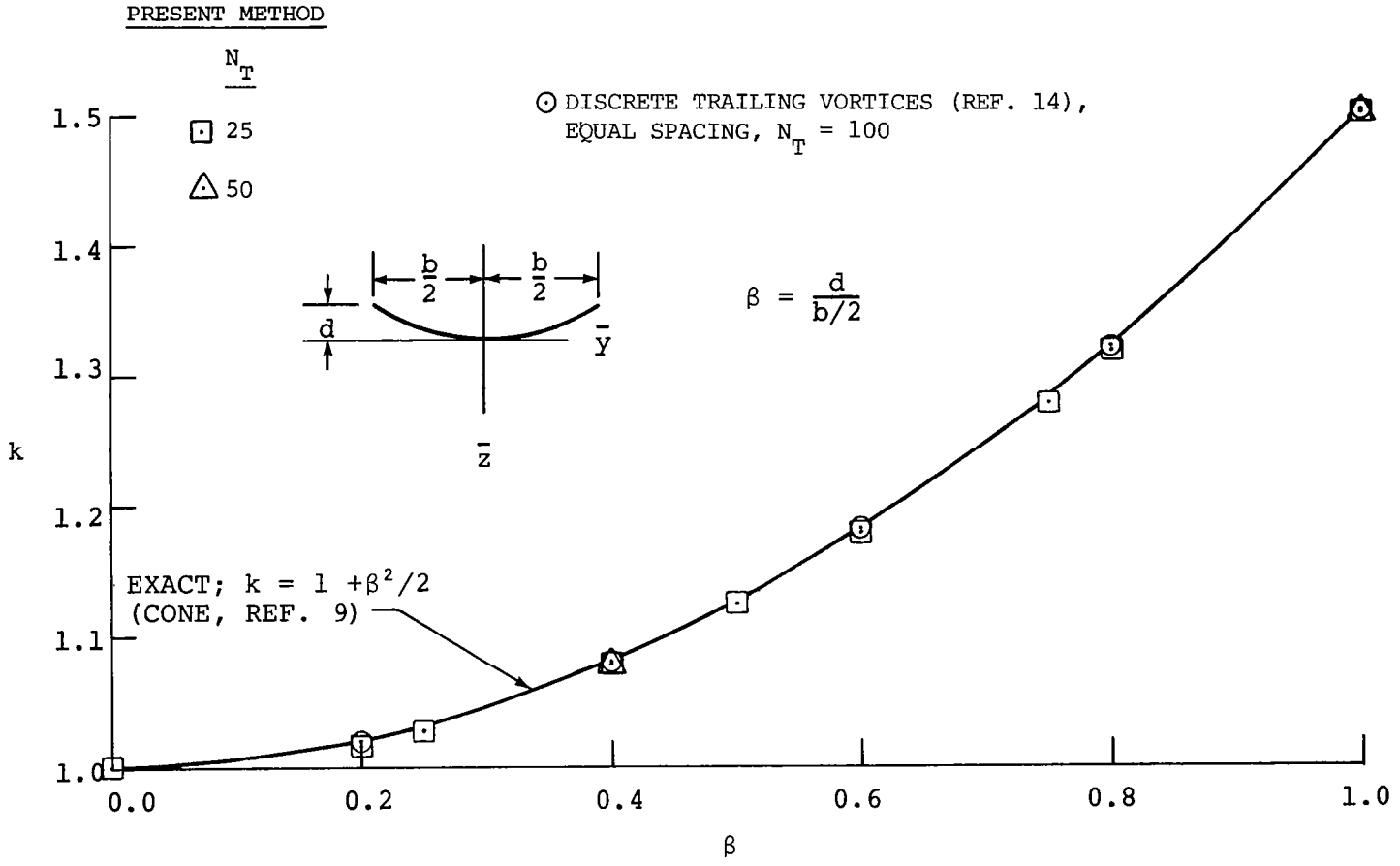

Figure 8. Induced drag efficiency factor for circular arc dihedral wings.

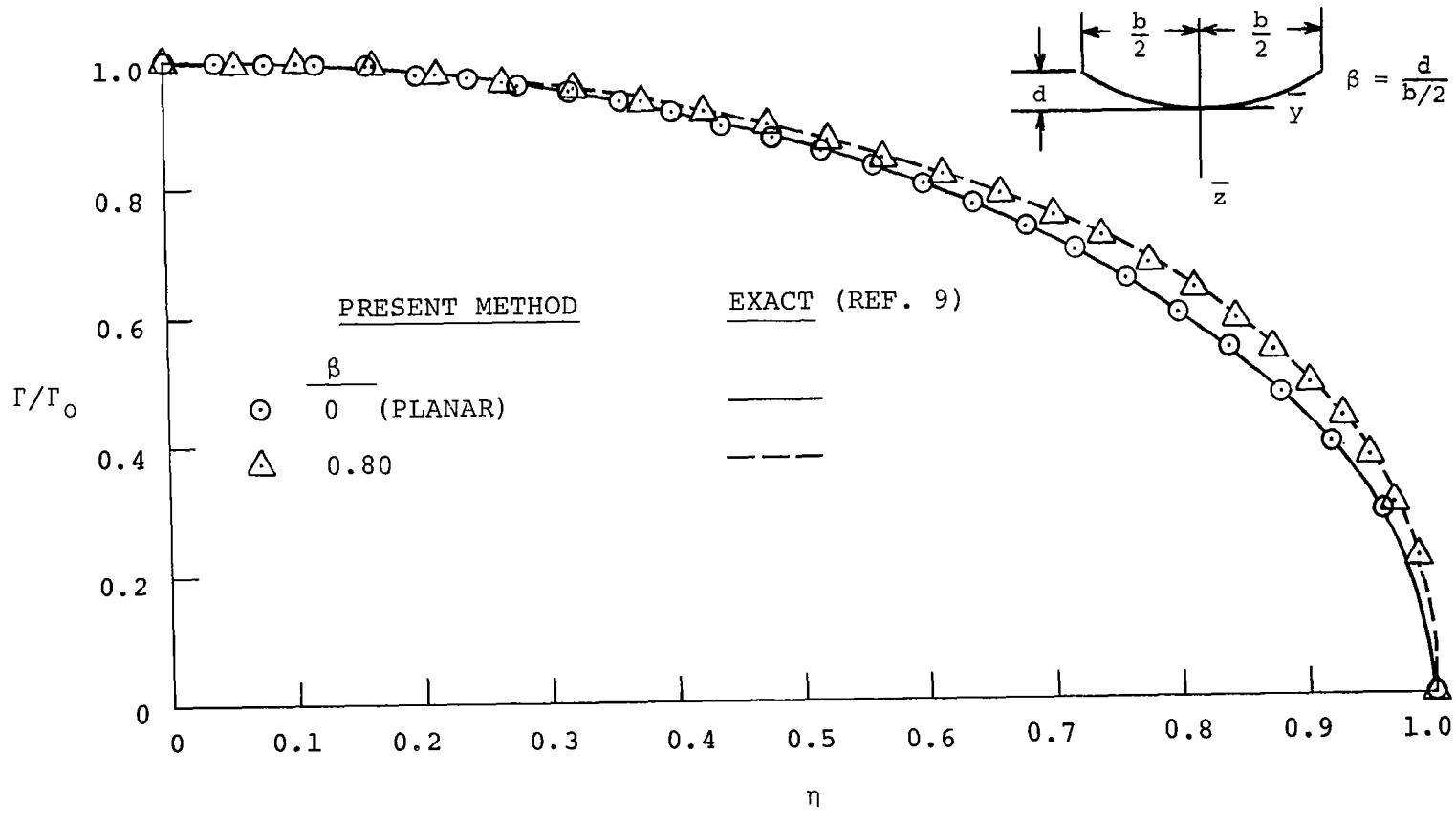

Figure 9. Effect of circular arc dihedral on the bound circulation distribution at minimum induced drag, $N_T = 25$.